

# $A^0 Z^0$ associated production at the Large Hadron Collider in the minimal supersymmetric standard model \*

Yin Jun<sup>2</sup>, Ma Wen-Gan<sup>1,2</sup>, Zhang Ren-You<sup>2</sup>, and Hou Hong-Sheng<sup>2</sup>

<sup>1</sup> CCAST (World Laboratory), P.O.Box 8730, Beijing 100080, P.R.China

<sup>2</sup> Department of Modern Physics, University of Science and Technology of China (USTC), Hefei, Anhui 230027, P.R.China

## Abstract

We investigate in detail the  $A^0 Z^0$  associated production process  $pp \rightarrow A^0 Z^0 + X$  within the framework of the minimal supersymmetric standard model (MSSM) at the CERN Large Hadron Collider (LHC), considering both contributions from the Drell-Yan and gluon fusion subprocesses. We focus on the deviations from the general two-Higgs-doublet model (2HDM) arising in the MSSM. We also discuss the contributions of the two  $A^0 Z^0$  associated production subprocesses in the MSSM at the LHC, and analyse the dependences of the total cross section on neutral CP-odd Higgs boson mass  $m_A$  and  $\tan\beta$  in the mSUGRA scenario. We find that the contribution from loop mediated gluon fusion subprocess can be competitive with that from the Drell-Yan subprocess in some parameter space.

PACS: 12.15Lk, 12.60.Jv, 12.60.Fr, 13.85 -t ,14.80.Cp

---

\*Supported by National Natural Science Foundation of China.

# I Introduction

The minimal standard model(MSM) [1] [2] has been proved by all precise experimental data that the MSM is a very successful model of particle physics. But until now the symmetric breaking structure of the electroweak interactions has not yet been directly explored experimentally. So the exploration of the SM Higgs boson is a major goal of the present and future colliders. As we know, any enlargement of the Higgs sector beyond the single  $SU(2)_L$  Higgs doublet of the MSM necessarily introduces other neutral Higgs bosons and charged Higgs bosons. Like the general two-Higgs-doublet model(2HDM), the minimal supersymmetric standard model (MSSM) [3] [4] requires the introduction of two Higgs doublets in order to preserve supersymmetry. These two Higgs doublets predict some more elementary Higgs bosons: one CP-even neutral Higgs boson( $H^0$ ), one CP-odd neutral Higgs boson( $A^0$ ) and two charged Higgs bosons( $H^\pm$ ), which are absent in the MSM. Any experimental discovery of these non-SM-like Higgs bosons will be the direct verification of these extended versions of the Higgs sector. Therefore, the study of various production mechanisms of the non-SM-like Higgs bosons at the present and future colliders is well motivated.

Searching for the non-SM-like Higgs bosons and studying their properties at the future multi-TeV hadron colliders, such as the CERN Large Hadron Collider (LHC), are possible as expected by supersymmetric (SUSY) theory [3] [5]. The gluon fusion mechanism  $gg \rightarrow \phi(\phi = h^0, H^0, A^0)$  provides the dominant production mechanism of neutral Higgs bosons at the LHC in the entire relevant mass range up to about 1 TeV for the small and moderate values of  $\tan \beta$  in the MSSM

[6]. The heavy neutral Higgs boson can be also produced in pair ( $A^0A^0, A^0h^0, A^0H^0$ ) at the LHC, if it is kinematically allowed [7]. Studying the process of a heavy charged Higgs boson associated with  $W$  boson is another attractive way in searching for the  $H^\pm$  bosons, because the  $W^\pm$ -boson's leptonic decay may be used as a spectacular trigger. The calculations of the heavy  $H^\pm$  production associated with  $W^\mp$  boson at a future electron-positron collider can be found in Refs. [8] [9] [10] [11] [12]. The complete calculations of the  $H^\pm W^\mp$  associated production at hadron colliders both in the 2HDM and the MSSM are given in Refs. [13] [14] [15] [16] [17]. Analogously,  $A^0 Z^0$  associated production would also be an efficient way in searching for the heavy neutral CP-odd Higgs boson  $A^0$ . Although the  $A^0$  boson can be produced in pair at future colliders [7] [18], the  $A^0 Z^0$  associated production will be the kinematically favored mechanism to produce  $A^0$  Higgs boson for the heavy  $A^0$  Higgs boson. And again the leptonic decay of  $Z^0$  maybe benefit for triggering the  $Z^0 A^0$  associated production events. The calculations of the  $Z^0 A^0$  associated production at a electron-positron collider were presented in Refs. [19] [20], at a muon collider in Ref. [21] and at a photon collider in Ref. [22], respectively. And Chung Kao gave the calculation of  $A^0 Z^0$  associated production via  $gg$  fusion including only quark loop diagrams at the SSC [23].

In this paper we concentrate on studying the  $A^0 Z^0$  associated production at the LHC in the MSSM, considering both subprocesses  $q\bar{q} \rightarrow A^0 Z^0$  and  $gg \rightarrow A^0 Z^0$ . In the calculation of the loop mediated process  $pp \rightarrow gg \rightarrow A^0 Z^0$ , we compare and discuss the cross sections in the general two-Higgs-doublet model (2HDM) and the MSSM. In section II, we present the calculation of the processes  $pp \rightarrow q\bar{q} \rightarrow A^0 Z^0$  and  $pp \rightarrow gg \rightarrow A^0 Z^0$ . Numerical results and

discussion are given in section III. There we use the MSSM parameters constrained within the minimal supergravity (mSUGRA) scenario [24]. Finally, a short summary is given.

## II Cross Section Calculation

In our calculation we use the t'Hooft-Feynman gauge and adopt the dimension regularization scheme in the general 2HDM and the dimensional reduction (DR) scheme [25] in the MSSM. In the loop diagram calculation we adopted the definitions of one-loop integral functions in reference [26]. The numerical calculation of the vector and tensor loop integral functions can be traced back to scalar loop integrals as shown in the reference[27]. The Feynman diagrams and the relevant amplitudes are created by FeynArts package automatically [28]. The numerical calculation of the loop integrals are implemented by using Mathematica programs.

### II.1 Calculation of the subprocess $q\bar{q} \rightarrow A^0 Z^0 + X$

We denote the  $A^0 Z^0$  associated production via Drell-Yan subprocess as

$$q(p_1) + \bar{q}(p_2) \rightarrow Z^0(k_1) + A^0(k_2), \quad (2.1)$$

Due to the feature of the Yukawa coupling that the coupling strength between quarks and Higgs boson is in proportion to the correspondent quark mass, the cross sections of subprocesses  $q\bar{q} \rightarrow A^0 Z^0 (q = u, d, s, c)$  should be much smaller than those of the subprocesses  $t\bar{t}(b\bar{b}) \rightarrow A^0 Z^0$ . Considering the fact that the luminosity of top (anti-top) quark is much lower than that of bottom (anti-bottom) quark from a proton, we conclude that the cross section of the process  $pp \rightarrow q\bar{q} \rightarrow A^0 Z^0 + X$  is approximately equal to the cross section of  $pp \rightarrow b\bar{b} \rightarrow A^0 Z^0 + X$ .

Therefore, in this paper we consider only the contributions from the  $pp \rightarrow b\bar{b} \rightarrow A^0 Z^0 + X$  process.

The Feynman diagrams of the subprocess  $b\bar{b} \rightarrow A^0 Z^0$  at the lowest order are depicted in Fig.1. The differential cross section of the subprocess  $b\bar{b} \rightarrow A^0 Z^0$  can be expressed as

$$d\hat{\sigma}_{b\bar{b}} = dP_{2f} \frac{1}{12} \sum_{spin} |A_{(a)}(\hat{s}, \hat{t}, \hat{u}) + A_{(b)}(\hat{s}, \hat{t}, \hat{u})|^2, \quad (2.2)$$

where the summation is taken over the spins of the initial and final states, and  $dP_{2f}$  denotes the two-particle phase space element. The factor  $1/12$  in above equation comes from the averaging over the spins and the colors of the incoming partons. The matrix element  $A_{(a)}$  represents the amplitude of the  $h^0(H^0)$  exchanging s-channel diagrams (shown in Fig.1(a)),  $A_{(b)}$  corresponds to the amplitude of u- and t-channel diagrams (shown in Fig.1(b)). The Mandelstam kinematical variables are defined as

$$\hat{s} = (p_1 + p_2)^2, \quad \hat{t} = (p_1 - k_1)^2, \quad \hat{u} = (p_1 - k_2)^2, \quad (2.3)$$

By using the relevant Feynman rules, we obtain the explicit expressions of these amplitudes:

$$\begin{aligned} A_{(a)}(\hat{s}, \hat{t}, \hat{u}) &= -\frac{(4\pi\alpha)m_b}{4s_W^2 c_W^2} \cos(\beta - \alpha) \frac{\sin \alpha}{\cos \beta} \epsilon^\mu(k_1) [\bar{v}(p_2)u(p_1)] \frac{(k_1 + p_1 + p_2)^\mu}{\hat{s} - m_h^2 + m_h \Gamma_h i} \\ &\quad - \frac{(4\pi\alpha_s)m_b}{4s_w^2 c_W^2} \sin(\beta - \alpha) \frac{\cos \alpha}{\cos \beta} \epsilon^\mu(k_1) [\bar{v}(p_2)u(p_1)] \frac{(k_1 + p_1 + p_2)^\mu}{\hat{s} - m_H^2 + m_H \Gamma_H i} \\ A_{(b)}(\hat{s}, \hat{t}, \hat{u}) &= -\frac{(4\pi\alpha)m_b}{2m_W s_W^2 c_W} \tan \beta \epsilon^\mu(k_1) \frac{1}{\hat{t} - m_b^2} \left[ \bar{v}(p_2) \gamma^5 (m_b - \not{k}_1 + \not{p}_1) \gamma^\mu \left( \frac{s_W^2}{3} - \frac{P_L}{2} \right) u(p_1) \right] \\ &\quad - \frac{(4\pi\alpha)m_b}{2m_W s_W^2 c_W} \tan \beta \epsilon^\mu(k_1) \frac{1}{\hat{u} - m_b^2} \left[ \bar{v}(p_2) \gamma^5 (m_b + \not{k}_1 - \not{p}_2) \gamma^\mu \left( \frac{s_W^2}{3} - \frac{P_L}{2} \right) u(p_1) \right] \end{aligned} \quad (2.4)$$

where  $m_b$  and  $m_W$  represent the masses of bottom quark and W boson, respectively.

## II.2 Calculation of the subprocess $gg \rightarrow A^0 Z^0 + X$

We denote the  $A^0 Z^0$  associated production process via gluon fusions as

$$g(p_1, \alpha) + g(p_2, \beta) \rightarrow Z^0(k_1) + A^0(k_2), \quad (2.5)$$

where  $\alpha, \beta$  are the color indices of initial gluons. As the subprocess  $gg \rightarrow Z^0 A^0$  is loop-induced, the one-loop order calculation can be simply carried out by summing all unrenormalized reducible and irreducible one-loop diagrams and the results will be finite and gauge invariant. We denote  $\sigma_{gg}^{2HDM}$  and  $\sigma_{gg}^{MSSM}$  as the cross sections in the framework of the general 2HDM and the MSSM, respectively. The former is contributed by the Feynman diagrams involving only the quark loop diagrams (shown in Fig.2) and the latter involves the contributions of both the quark and squark loop diagrams (shown in Fig.2-3). The possible corresponding Feynman diagrams created by exchanging the initial gluons or the two final states, should be also included in Fig.2 and Fig.3 and involved in our calculation.

We can see that each Feynman diagram in Fig.2 and Fig.3 contains one interacting vertex between (s)quarks and a Higgs boson. Due to the feature of the Yukawa coupling as we mentioned above, we can consider only the diagrams which involve the third generation (s)quark in the calculation of the subprocess  $gg \rightarrow A^0 Z^0$ . The cross sections of the subprocess  $gg \rightarrow A^0 Z^0$  in the general 2HDM and the MSSM can be expressed respectively as

$$\begin{aligned} d\hat{\sigma}_{gg}^{2HDM} &= dP_{2f} \frac{1}{256} \sum |A_{(a)}^{(2)}(\hat{s}, \hat{t}, \hat{u}) + A_{(b)}^{(2)}(\hat{s}, \hat{t}, \hat{u}) + A_{(c)}^{(2)}(\hat{s}, \hat{t}, \hat{u})|^2 \\ d\hat{\sigma}_{gg}^{MSSM} &= dP_{2f} \frac{1}{256} \sum |A_{(a)}^{(2)}(\hat{s}, \hat{t}, \hat{u}) + A_{(b)}^{(2)}(\hat{s}, \hat{t}, \hat{u}) + A_{(c)}^{(2)}(\hat{s}, \hat{t}, \hat{u}) \\ &\quad + A_{(a)}^{(3)}(\hat{s}, \hat{t}, \hat{u}) + A_{(b)}^{(3)}(\hat{s}, \hat{t}, \hat{u}) \cdots + A_{(g)}^{(3)}(\hat{s}, \hat{t}, \hat{u})|^2 \end{aligned} \quad (2.6)$$

where the summation is taken over the spins and colors of the initial and final states, and  $dP_{2f}$  denotes the two-particle phase space element.  $A_{(j)}^{(i)}$  represents the amplitude of the diagram of Fig.i(j). The factor  $1/256$  results from the averaging over the spins and the colors of the incoming partons.

### II.3 Cross section of $pp \rightarrow A^0 Z^0 + X$ process at the LHC

With the cross sections of the related subprocesses, the cross section of parent process  $pp \rightarrow A^0 Z^0 + X$  at the proton-proton collider LHC can be obtained by doing the following integration,

$$\sigma_{ij} = \int_{(m_Z+m_A)^2/s}^1 d\tau \frac{d\mathcal{L}_{ij}}{d\tau} \hat{\sigma}_{ij}(\hat{s} = \tau s) \quad (2.7)$$

where

$$\frac{d\mathcal{L}_{ij}}{d\tau} = \frac{1}{1 + \delta_{ij}} \int_{\tau}^1 \frac{dx_1}{x_1} \left\{ \left[ f_{i/p}(i, x_1, Q^2) f_{j/p}(j, \frac{\tau}{x_1}, Q^2) \right] + \left[ f_{j/p}(j, x_1, Q^2) f_{i/p}(i, \frac{\tau}{x_1}, Q^2) \right] \right\} \quad (2.8)$$

In Eq.(2.7)  $\sqrt{s}$  and  $\sqrt{\hat{s}}$  are the colliding proton-proton and parton-parton c.m.s. energies respectively. The notation  $\sigma_{ij}$  represents the cross section of the parent process  $pp \rightarrow ij \rightarrow A^0 Z^0 + X$ .  $d\mathcal{L}_{ij}/d\tau$  is the luminosity of incoming partons where  $i, j$  can be  $b, \bar{b}$  and  $g$ ,  $\tau = x_1 x_2$ .  $m_Z$  and  $m_A$  represent the masses of  $Z^0$  boson and  $A^0$  Higgs boson. The definitions of  $x_1$  and  $x_2$  can be found in Ref.[29]. In our calculation, we adopt the CTEQ5 parton distribution function [30] and take the factorization scale  $Q$  to be  $\sqrt{\hat{s}}$ . The Eq.(2.7) can be rewritten as

$$\sigma_{ij} = \int_{m_Z+m_A}^{\sqrt{\hat{s}}} d\sqrt{\hat{s}} \hat{\sigma}_{ij}(\hat{s}) H_{ij}(\hat{s}) \quad (2.9)$$

where

$$H_{ij}(\hat{s}) = \frac{1}{1 + \delta_{ij}} \int_{\frac{\hat{s}}{s}}^1 \frac{2dx_1 \sqrt{\hat{s}}}{x_1 s} \left\{ \left[ f_{i/p}(i, x_1, Q^2) f_{j/p}(j, \frac{\hat{s}}{x_1 s}, Q^2) \right] + (i \leftrightarrow j) \right\} \quad (2.10)$$

When  $ij = gg$ ,  $\sigma_{gg}^{2HDM}$  represents the cross section of the parent process  $pp \rightarrow gg \rightarrow A^0 Z^0 + X$  contributed only by quark loop diagrams shown in Fig.2, while  $\sigma_{gg}^{MSSM}$  represents the cross section contributed by both quark and squark loop diagrams shown in Fig.2 and Fig.3. In the next section we shall take different input data sets to demonstrate the production rates of the parent process  $pp \rightarrow A^0 Z^0 + X$ . The numerical results of  $\sigma_{gg}^{2HDM}$  and  $\sigma_{gg}^{MSSM}$  would show the importance of squark loop diagrams. The total cross section of  $pp \rightarrow A^0 Z^0 + X$  at proton-proton collider should be the summation of  $\sigma_{b\bar{b}}$  and  $\sigma_{gg}$ . Quantitatively comparing the  $\sigma_{b\bar{b}}$  with  $\sigma_{gg}$  will help us to know in which part of the parameter space the contribution of gluon-gluon fusion process is dominant.

### III Numerical result and discussion

#### III.1 Input parameters

In the numerical calculation, we take the SM parameters as:  $m_t = 174.3$  GeV,  $m_b = 4.2$  GeV,  $m_Z = 91.187$  GeV,  $\Gamma_Z = 2.49$  GeV [31], and take the supersymmetric parameters being constrained within the minimal supergravity (mSUGRA) scenario [24]. In this scenario, only five supersymmetric parameters should be inputted, namely  $M_{1/2}$ ,  $M_0$ ,  $A_0$ , sign of  $\mu$  and  $\tan \beta$ , where  $M_{1/2}$ ,  $M_0$  and  $A_0$  are the universal gaugino mass, scalar mass at GUT scale and the trilinear soft breaking parameter in the superpotential terms, respectively. In this work, we take  $M_{1/2}=120$  GeV,  $A_0=300$  GeV and  $\mu > 0$ .  $M_0$  is obtained quantitatively from the input  $m_A$  value. All other MSSM parameters are determined in the mSUGRA scenario by using program package ISAJET 7.44. In this program, the renormalization group equations (RGE's) [32] are run from

the weak scale  $m_Z$  up to the GUT scale, taking all thresholds into account in order to get the low energy scenario from the mSUGRA. It uses two loop RGE's only for the gauge couplings and the one-loop RGE's for the other supersymmetric parameters. The GUT scale boundary conditions are imposed and the RGE's are run back to  $m_Z$ , again taking threshold into account.

Here we give some comments about the choice of the decay width values of CP-even neutral Higgs bosons  $h^0$  and  $H^0$ . We know that some of the Feynman diagrams (shown in Fig.1-3) have s-channel  $h^0$  and  $H^0$  propagators, which have analytical expressions respectively as

$$\frac{1}{\hat{s} - m_h^2 + im_h\Gamma_h} = \frac{\hat{s} - im_h^2 - m_h\Gamma_h}{(\hat{s} - m_h^2)^2 + m_h^2\Gamma_h^2}, \quad (3.1)$$

$$\frac{1}{\hat{s} - m_H^2 + im_H\Gamma_H} = \frac{\hat{s} - m_H^2 - im_H\Gamma_H}{(\hat{s} - m_H^2)^2 + m_H^2\Gamma_H^2}, \quad (3.2)$$

It is clear that the cross sections of the subprocess should be related to the decay widths of  $h^0$  and  $H^0$ . In this work the input parameter  $m_A$  is taken in the range of 200 GeV to 650 GeV. Then we have the following constraints in this parameter space,

$$m_H \approx m_A, \quad m_h < 150 \text{ GeV}, \quad (3.3)$$

and by using the package HDECAY[33] in the MSSM, we find

$$\Gamma_H, \Gamma_h < 10 \text{ GeV}. \quad (3.4)$$

Because  $\sqrt{\hat{s}} \geq m_A + m_Z$ , we get  $(\hat{s} - m_H^2)^2 \gg m_H^2\Gamma_H^2$ . The propagator of  $H^0$  boson can be expressed approximately as

$$\frac{\hat{s} - m_H^2 - im_H\Gamma_H}{(\hat{s} - m_H^2)^2 + m_H^2\Gamma_H^2} \approx \frac{1}{(\hat{s} - m_H^2)} \quad (3.5)$$

It is obvious that the bigger the  $\sqrt{\hat{s}}$  is, the less sensitive the cross section to the decay widths of neutral Higgs bosons  $H^0$  and  $h^0$  is. Therefore, we choose  $\Gamma_H = \Gamma_h = 10$  GeV in our numerical calculations. Actually, our final numerical result of the cross section of the process  $pp \rightarrow A^0 Z^0 + X$  at the LHC, shows also that it is not sensitive to the choice of these two decay widths.

### III.2 Discussion and analysis

The figures in Fig.4, Fig.5 and Fig.6, show the cross sections (or differential cross sections) of the process  $pp \rightarrow gg \rightarrow A^0 Z^0 + X$  at the LHC as the functions of the CP-odd Higgs boson  $A^0$  mass, the ratio of the vacuum expectation values  $\tan \beta$  and the transverse momentum  $p_T$ , respectively. The curves of the cross sections (or differential cross sections) involving the contributions from quark loop diagrams (in the general 2HDM) and quark+squark loop diagrams (in the MSSM) are depicted separately on these figures for comparison of the cross sections in these two models. And in these three figures the full-lines are for  $\sigma_{gg}^{2HDM}$  (or  $d\sigma_{gg}^{2HDM}/dp_T$ ), the dotted-lines are for  $\sigma_{gg}^{MSSM}$  (or  $d\sigma_{gg}^{MSSM}/dp_T$ ).

Figure 4 shows the relationship between the cross section of the parent process  $pp \rightarrow gg \rightarrow A^0 Z^0 + X$  and  $m_A$  with the colliding energy  $\sqrt{s} = 14$  TeV. The input mSUGRA parameters are set to be the typical values mentioned in the last subsection (i.e.  $M_{1/2}=120$  GeV,  $A_0=300$  GeV and  $\mu > 0$ .  $M_0$  is obtained quantitatively from the  $m_A$  value), and  $\tan \beta=2, 7$  and  $32$ , respectively. From this figure, we find that in some parameter space the scalar quark contributions can enhance the cross section obviously, that is to say  $\sigma_{gg}^{MSSM} > \sigma_{gg}^{2HDM}$ , while in other regions, we have  $\sigma_{gg}^{MSSM} < \sigma_{gg}^{2HDM}$ . The figure shows that when we have small and

moderate  $\tan\beta$  values, the scalar quark loop contribution to the  $A^0Z^0$  associated production at the LHC is most obvious. We shall also see later from Fig.7 that when  $\tan\beta$  has small or moderate value, the contributions from gluon fusion subprocess is dominant. Therefore, it is possible to use the experimental measurement of the  $A^0Z^0$  associated production at the LHC to disentangle the MSSM from the general 2HDM in these parameter space regions.

In Fig.5, the cross section of the parent process  $pp \rightarrow gg \rightarrow A^0Z^0 + X$  at the LHC versus  $\tan\beta$  is plotted. The values of the neutral CP-odd Higgs boson  $A^0$  mass are set to be 200 GeV, 400 GeV and 600 GeV, respectively. From the figure, we also find that scalar quark contributions can either enhance or suppress the cross section of the parent process as shown in Fig.4. Fig.5 together with Fig.4, show that when the value of  $m_A$  is greater than 400 GeV and  $\tan\beta < 8$ , the contribution from the scalar quark loop diagrams increases with the decrement of  $\tan\beta$ . In Fig.5 the two curves for  $m_A = 400$  GeV and 600 GeV demonstrate that when  $\tan\beta < 8$ , the scalar quark contribution suppresses the cross section, which means  $\sigma_{gg}^{MSSM} < \sigma_{gg}^{2HDM}$ , and while the scalar quark contribution enhances the cross section when  $\tan\beta > 20$ . These features can be also seen from Fig.4. The curve for  $\tan\beta = 2$  in Fig.4, demonstrates that  $\sigma_{gg}^{MSSM}$  is about two third of  $\sigma_{gg}^{2HDM}$  quantitatively, while the curve for  $\tan\beta = 32$  shows  $\sigma_{gg}^{MSSM} > \sigma_{gg}^{2HDM}$ .

Fig.6 displays the differential cross section  $d\sigma/dp_T$  of the process  $pp \rightarrow gg \rightarrow A^0Z^0$  at the LHC versus transverse momentum  $p_T$  with  $\sqrt{s} = 14$  TeV and the pseudo-rapidity being in the range of  $|\eta| < 2$ . The  $A^0$  mass is set to be 350 GeV, and  $\tan\beta$  is taken as 2, 7 and 32, respectively. We find that for  $\tan\beta = 2$ , the scalar quark contribution suppresses the differential cross section  $d\sigma/dp_T$ . For  $\tan\beta = 32$  and  $p_T > 100$  GeV, the scalar quark contribution enhances

the differential cross section. But for  $\tan\beta = 7$ , the scalar quark contribution can either enhance or suppress the differential cross section in different  $p_T$  regions.

In Fig.7, Fig.8 and Fig.9, we plot the the cross sections of the process  $pp \rightarrow b\bar{b} \rightarrow A^0 Z^0 + X$  ( $\sigma^{(DY)}$ ), and the process  $pp \rightarrow A^0 Z^0 + X$  contributions from both Drell-Yan and gluon-gluon fusion subprocesses in the constrained MSSM ( $\sigma^{(T)} = \sigma^{(DY)} + \sigma_{gg}^{MSSM}$ ), as the functions of the CP-odd Higgs boson  $A^0$  mass, the ratio of the vacuum expectation values  $\tan\beta$  and the transverse momentum  $p_T$ , respectively. In these three figures, the full-lines are for the cross sections or differential cross sections of the process  $pp \rightarrow b\bar{b} \rightarrow A^0 Z^0 + X$  via Drell-Yan subprocess, the dotted-lines are for the process  $pp \rightarrow A^0 Z^0 + X$  via both Drell-Yan and gluon fusion subprocesses. With the comparison between the  $\sigma^{(T)}$  (or  $d\sigma^{(T)}/dp_T$ ) and  $\sigma^{(DY)}$  (or  $d\sigma^{(DY)}/dp_T$ ), we can know in which parameter space in the constrained MSSM, the contribution from the loop mediated subprocess  $gg \rightarrow A^0 Z^0$  is important.

Fig.7 displays the cross sections of  $pp \rightarrow b\bar{b} \rightarrow A^0 Z^0 + X$  and  $pp \rightarrow A^0 Z^0 + X$  at proton-proton colliders versus the mass of  $A^0$  with  $\sqrt{s} = 14$  TeV. We choose  $\tan\beta=2, 7$  and  $32$ , respectively. From Fig.7, we find that in the region of  $\tan\beta \leq 7$ , the contribution of gluon-gluon fusion subprocess in the MSSM enhances the cross section, especially when  $\tan\beta = 2$  the contribution of the gluon-gluon fusion subprocess is about 80% of the total cross section  $\sigma^{(T)}$ . In fact, the gluon-gluon fusion subprocess is the most important  $A^0 Z^0$  associated production mechanism in this parameter space. From the figure we see also that when  $\tan\beta=32$  the difference between  $\sigma^{(DY)}$  and  $\sigma^{(T)}$  is very small, it means that the contribution of the gluon-gluon fusion subprocess is negligible in this parameter space.

The cross sections of  $pp \rightarrow b\bar{b} \rightarrow A^0 Z^0 + X$  and  $pp \rightarrow A^0 Z^0 + X$  at the LHC as the functions of  $\tan\beta$  with  $\sqrt{s} = 14 \text{ TeV}$  are shown in Fig.8. The mass of Higgs boson  $A^0$  is taken as 200 GeV, 400 GeV and 600 GeV, respectively. From this figure we can find also that gluon-gluon fusion subprocess enhances the cross section of the  $A^0 Z^0$  associated production at the LHC, and will become a very important production mechanism when  $\tan\beta < 10$ . In the region of  $\tan\beta > 10$ , the cross section of the  $A^0 Z^0$  associated production at the LHC are in the range of  $1 - 10^2 \text{ fb}$ . Even the  $\sigma^{(T)}$  can reach 300 fb when  $\tan\beta = 48$  and  $m_A = 200 \text{ GeV}$ . So the  $A^0 Z^0$  associated production process may be easily observed experimentally if  $\tan\beta$  is large enough.

Fig.9 displays the differential cross sections ( $d\sigma/dp_T$ ) of  $pp \rightarrow A^0 Z^0 + X$  and  $pp \rightarrow b\bar{b} \rightarrow A^0 Z^0 + X$  at the LHC as the functions of the transverse momentum  $p_T$  with the pseudo-rapidity being in the range of  $|\eta| < 2$ . We choose  $m_A = 350 \text{ GeV}$ , and take  $\tan\beta=2, 7$  and  $32$ , respectively. From this figure we can see that at high  $p_T$  region, when  $\tan\beta \leq 7$ , the difference between  $d\sigma^{(DY)}/dp_T$  and  $d\sigma^{(T)}/dp_T$  is obvious, even when  $\tan\beta=2$ , the  $d\sigma^{(DY)}/dp_T$  can be less than 1% of  $d\sigma^{(T)}/dp_T$ , which means that the contribution from the  $pp \rightarrow gg \rightarrow A^0 Z^0 + X$  process is dominant in this parameter space. But when  $\tan\beta = 32$ , the contribution to the total differential cross sections ( $d\sigma^{(T)}/dp_T$ ) is mainly from the Drell-Yan  $A^0 Z^0$  associated production subprocess, and the contribution from gluon fusion subprocess is negligible.

## IV Summary

In this paper, we studied the neutral CP-odd Higgs boson  $A^0$  production with the association of  $Z^0$  gauge boson via both Drell-Yan and gluon-gluon fusion subprocesses in the constrained

MSSM at the CERN LHC. Numerical analysis of their production rates is carried out with some typical parameter sets in the mSUGRA scenario. Our results show that the cross section in the MSSM is clearly enhanced by the gluon-gluon fusion subprocess in the parameter space with small or moderate  $\tan\beta$  value, and we should consider the gluon-gluon fusion subprocess in this parameter space in the calculation of the  $A^0Z^0$  associated production at the LHC. We compared above results of the process  $pp \rightarrow gg \rightarrow A^0Z^0 + X$  in the MSSM with those in the general two-Higgs-doublet model (2HDM), where the cross section of subprocess  $gg \rightarrow A^0Z^0 + X$  is contributed only by quark loop diagrams. We find that the contributions from the scalar quark loops in the MSSM can either enhance or suppress the cross section obviously and cannot be neglected in some parameter space. The results show also that the  $A^0Z^0$  associated production at the LHC is strongly related to the parameters  $\tan\beta$  and the mass of  $A^0$ . The total cross section increases with increment of  $\tan\beta$ , and decreases with increment of  $m_A$ .

**Acknowledgments:** This work was supported in part by the National Natural Science Foundation of China and a grant from the Education Ministry of China .

## References

- [1] S. L. Glashow, Nucl. Phys. **22** (1961) 579; S. Weinberg, Phys. Rev. Lett. **1** (1967) 1264; A. Salam, Proc. 8th Nobel Symposium Stockholm 1968, ed. N. Svartholm(Almquist and Wiksells, Stockholm 1968) p.367; H. D. Politzer, Phys. Rep. **14** (1974) 129.
- [2] P. W. Higgs, Phys. Lett **12** (1964) 132, Phys. Rev. Lett. **13** (1964) 508; Phys. Rev. **145** (1966) 1156; F. Englert and R.Brout, Phys. Rev. Lett. **13** (1964) 321; G. S. Guralnik, C.

- R. Hagen and T. W. B. Kibble, Phys. Rev. Lett. **13** (1964) 585; T. W. B. Kibble, Phys. Rev. **155** (1967) 1554.
- [3] H. E. Haber and G. L. Kane, Phys. Rep. **117** (1985) 75.
- [4] J. F. Gunion, H. E. Haber, G. L. Kane and S. Dawson, The Higgs Hunter's Guide (Addison-Wesley, Reading 1990).
- [5] H. Nilles, Phys. Rep. **110** (1984) 1; J. Rosiek, Phys. Rev. **D41** (1990) 3464, hep-ph/9511250(E); M. Kuroda, hep-ph/9902340.
- [6] J. F. Gunion, H. E. Haber and C. Kao, Phys. Rev. **D46**, 2907; M. Spira, Fortschr. Phys. **46** (1998)203; M. Spira, A. Djouadi, D. Graudenz and P. M. Zerwas, Nucl. Phys. **B453** (1995) 17.
- [7] A.A. Barrientos-Bendezu and B.A. Kniehl, Phys. Rev. **D64** (2001) 035006.
- [8] A. Arhrib, M.C. Peyranere, W. Hollik and G. Moultaka, Nucl. Phys. **B581** (2000) 34.
- [9] S. Kanemura, Eur. Phys. J. **C17** (2000) 473.
- [10] S.H. Zhu, hep-ph/9901221.
- [11] Heather E. Logan, Shufang Su, hep-ph/0203270.
- [12] F. Zhou, W.G. Ma, Y. Jiang, X.Q. Li and L.H. Wan, Phys. Rev. **D64** (2001) 055005.
- [13] D. A. Dicus, J. L. Hewett, C. Kao and T.G. Rizzo, Phys. Rev. **D40** (1989) 789.

- [14] A. A. Barrientos Bendezu and B.A. Kniehl, Phys. Rev. **D59** (1998) 015009.
- [15] A.A. Barrientos Bendezu and B.A. Kniehl, Phys. Rev. **D61** (2000) 097701.
- [16] F. Zhou, W.G. Ma, Y.Jiang, L. Han and L.H. Wan, Phys. Rev. **D62** (2000) 015002.
- [17] O. Brein, W. Hollik and S. Kanemura, Phys. Rev. **D63** (2001) 095001.
- [18] G.J. Gounaris, P.I. Porfyriadis, Eur. Phys. J. **C18** (2001) 181, hep-ph/0007110.
- [19] A.G. Akeroyd, A. Arhrib and M. Capdequi Peyranere, Mod. Phys. Lett. **A14** (1999) 2093;  
Mod. Phys. Lett. **A17** (2002) 373, hep-ph/9907542.
- [20] A.G. Akeroyd, A. Arhrib and M. Capdequi Peyranere, Phys. Rev. **D64** (2001) 075007;  
Phys. Rev. **D65** (2002) 099903, hep-ph/0104243.
- [21] A.G. Akeroyd, A. Arhrib and C. Dove, Phys. Rev. **D61** (2000) 071702.
- [22] G.J. Gounaris, P.I. Porfyriadis and F.M. Renard, Eur. Phys. J. **C20** (2001) 659.
- [23] Chung Kao, Phys. Rev. **D46** (1992) 4907, FSU-HEP-911205.
- [24] M. Drees and S.P. Martin, MAD-PH-879, UM-TH-95-02, hep-ph/9504324.
- [25] D.M. Copper, D.R.T. Jones, P. van Nieuwennuizen, Nucl. Phys. **B167** (1980) 479;
- [26] Bernd A. Kniehl, Phys. Rep. 240(1994)211.
- [27] G. Passarino and M. Veltman, Nucl. Phys. **B160**, 151(1979).

- [28] J. Küblbeck, M. Böhm and A. Denner, Comput. Phys. Commun. **60** (1990) 165; T. Hahn, hep-ph/9905354.
- [29] Y. Jiang, W.G. Ma, L. Han, Z.H. Yu and H. Pietschmann, Phys. Rev. **D62** (2000) 035006.
- [30] H.L. Lai, J. Huston, and S. Kuhlmann , Eur. Phys. J. **C12** (2000) 375, hep-ph/9903282.
- [31] D.E. Groom, et al., Euro. Phys. J. **C15**, (2000) 1; D. Schaile, CERN-PPE/94-162(11 October 1994).
- [32] V. Barger, M.S. Berger and P. Ohmann, Phys. Rev. **D47** (1993) 1093, **D47** (1993) 2038; V. Barger, M.S. Berger, P. Ohmann and R.J. N. Phillips, Phys. Lett. **B314** (1993) 351; V. Barger, M.S. berger and P. Ohmann, Phys. Rev. **D49** (1994) 4908.
- [33] M. Spira, Nucl. Instr. and Meth. in Phys. Res. **A389** (1997) 357; A. Djouadi, J. Kalinowski and M. Spira, Comput. Phys. Commun. **108** (1998) 56.

## Figure Captions

**Fig.1** The relevant Feynman diagrams for the subprocess  $b\bar{b} \rightarrow A^0 Z^0$  in the MSSM at the tree-level: (a) s-channel diagrams. (b) u- and t-channel diagrams. Note that Fig.1(b) includes the diagram created by exchanging two final states.

**Fig.2** The relevant Feynman diagrams for the subprocess  $gg \rightarrow Z^0 A^0$  at the one loop-level (including only the quark loop diagrams).

**Fig.3** The relevant Feynman diagrams for the subprocess  $gg \rightarrow A^0 Z^0$  at the one loop-level (including only the scalar quark loop diagrams).

**Fig.4** The cross sections  $\sigma_{gg}^{2HDM}$  and  $\sigma_{gg}^{MSSM}$  of the process  $pp \rightarrow gg \rightarrow A^0 Z^0 + X$ , as the functions of the mass of Higgs boson  $A^0$ . The input parameter  $\tan \beta$  is taken as 2, 7 and 32, respectively.

**Fig.5** The cross sections  $\sigma_{gg}^{2HDM}$  and  $\sigma_{gg}^{MSSM}$  of the process  $pp \rightarrow gg \rightarrow A^0 Z^0 + X$ , as the functions of  $\tan \beta$ . The mass of Higgs boson  $A^0$  is taken as 200 GeV, 400 GeV and 600 GeV, respectively.

**Fig.6** The differential cross sections  $d\sigma_{gg}^{2HDM}/dp_T$  and  $d\sigma_{gg}^{MSSM}/dp_T$  of the process  $pp \rightarrow gg \rightarrow A^0 Z^0 + X$ , as the functions of the transverse momentum  $p_T$  in the mSUGRA scenario at the LHC with  $\sqrt{s} = 14$  TeV,  $m_A = 350$  GeV and the pseudo-rapidity being in the range of  $|\eta| < 2$ . The ratio of the vacuum expectation values  $\tan \beta$  is taken as 2, 7 and 32, respectively.

**Fig.7** The cross sections  $\sigma^{(DY)}$  and  $\sigma^{(T)}$  of the process  $pp \rightarrow A^0 Z^0 + X$  as the functions of the mass of Higgs boson  $A^0$ , The ratio of the vacuum expectation values  $\tan \beta$  is taken as 2, 7 and 32, respectively.

**Fig.8** The cross sections  $\sigma^{(DY)}$  and  $\sigma^{(T)}$  of the process  $pp \rightarrow A^0 Z^0 + X$  as the functions of  $\tan \beta$ . The mass of Higgs boson  $A^0$  is taken as 200 GeV, 400 GeV and 600 GeV, respectively.

**Fig.9** The differential cross sections  $d\sigma^{(DY)}/dp_T$  and  $d\sigma^{(T)}/dp_T$  of the process  $pp \rightarrow A^0 Z^0 + X$ , as the functions of the transverse momentum  $p_T$  in the mSUGRA scenario with  $\sqrt{s} = 14$  TeV,  $m_A = 350$  GeV and the pseudo-rapidity being in the range of  $|\eta| < 2$ . The ratio of the vacuum expectation values  $\tan \beta$  is taken as 2, 7 and 32, respectively.

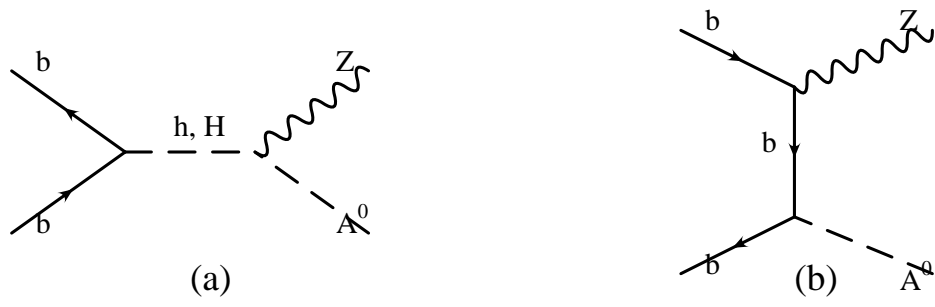


Figure. 1

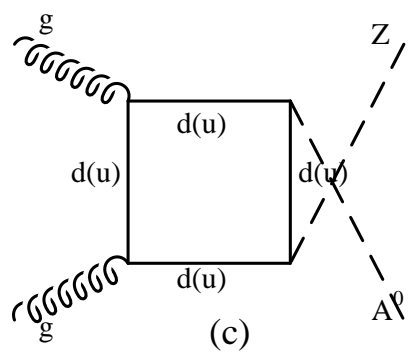
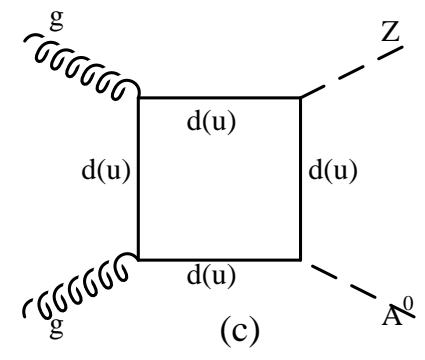
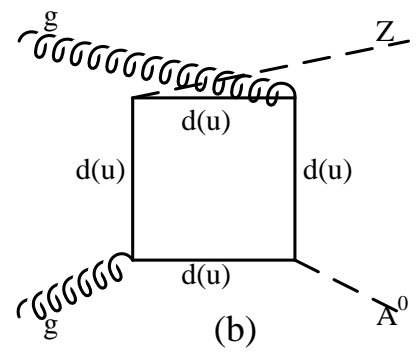
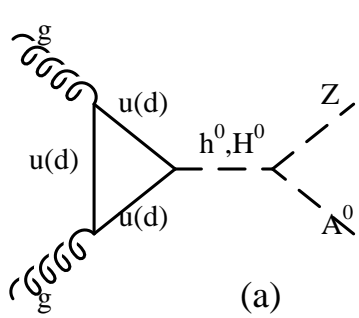


Figure. 2

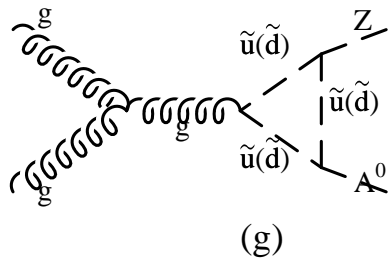
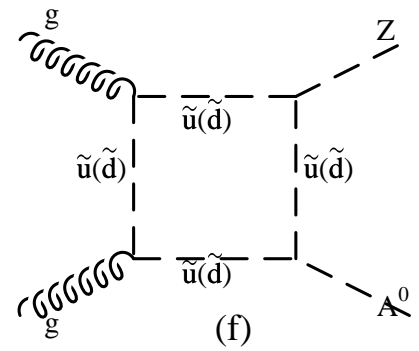
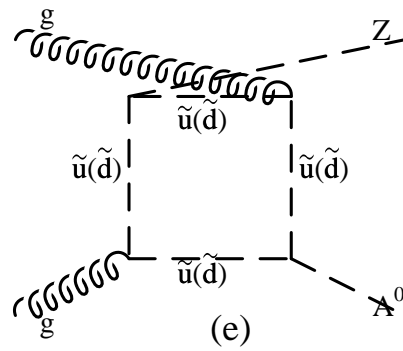
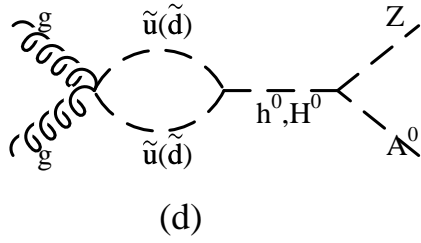
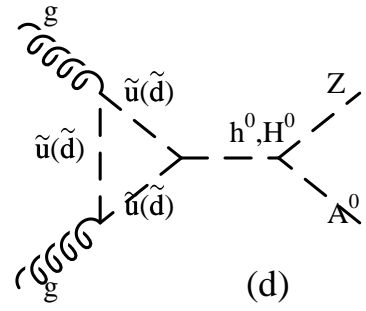
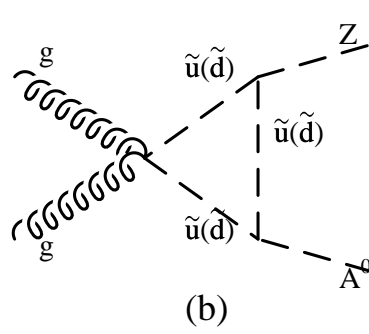
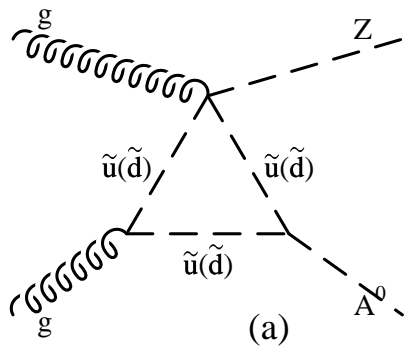


Figure. 3

Fig.4

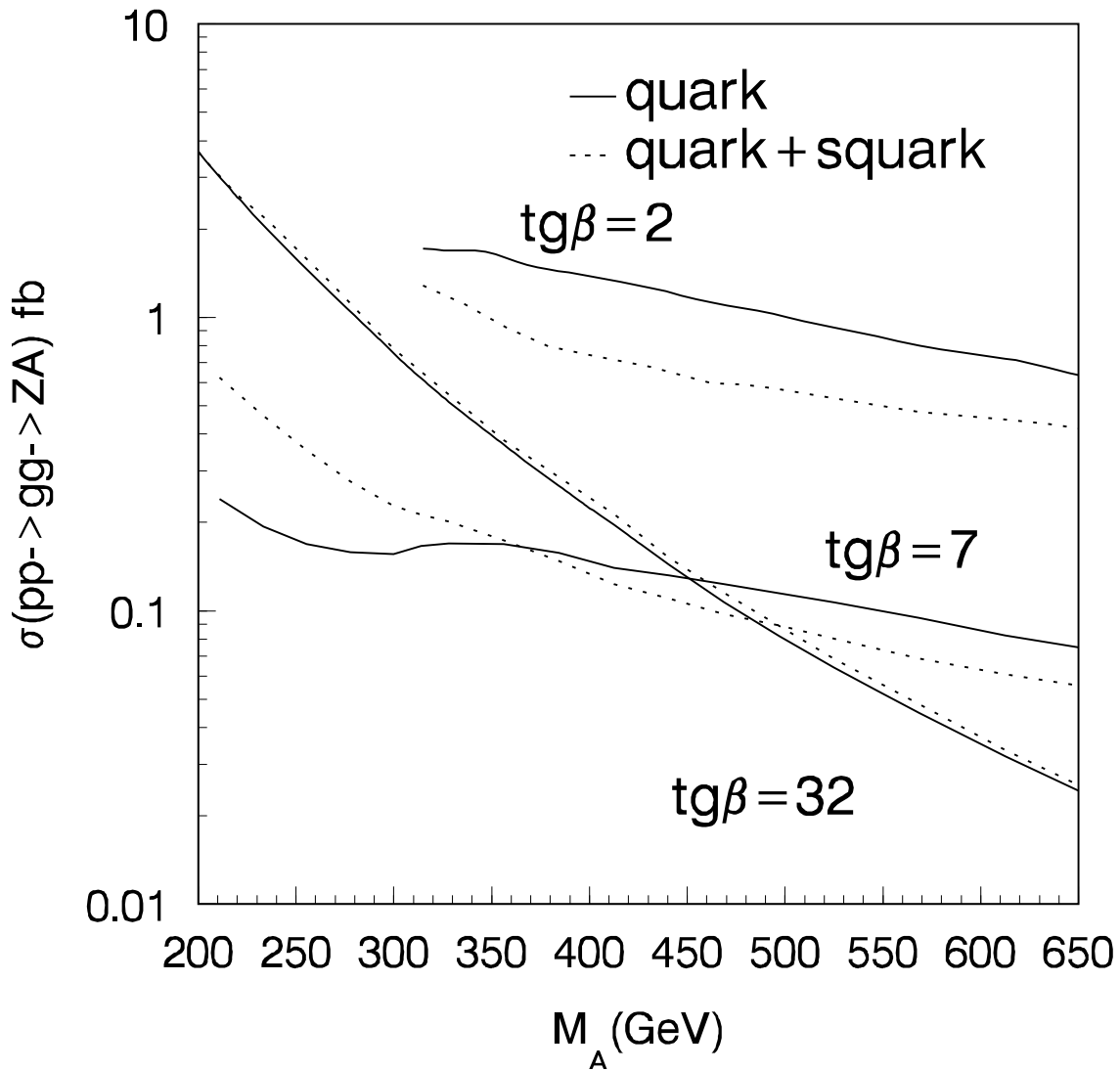


Fig.5

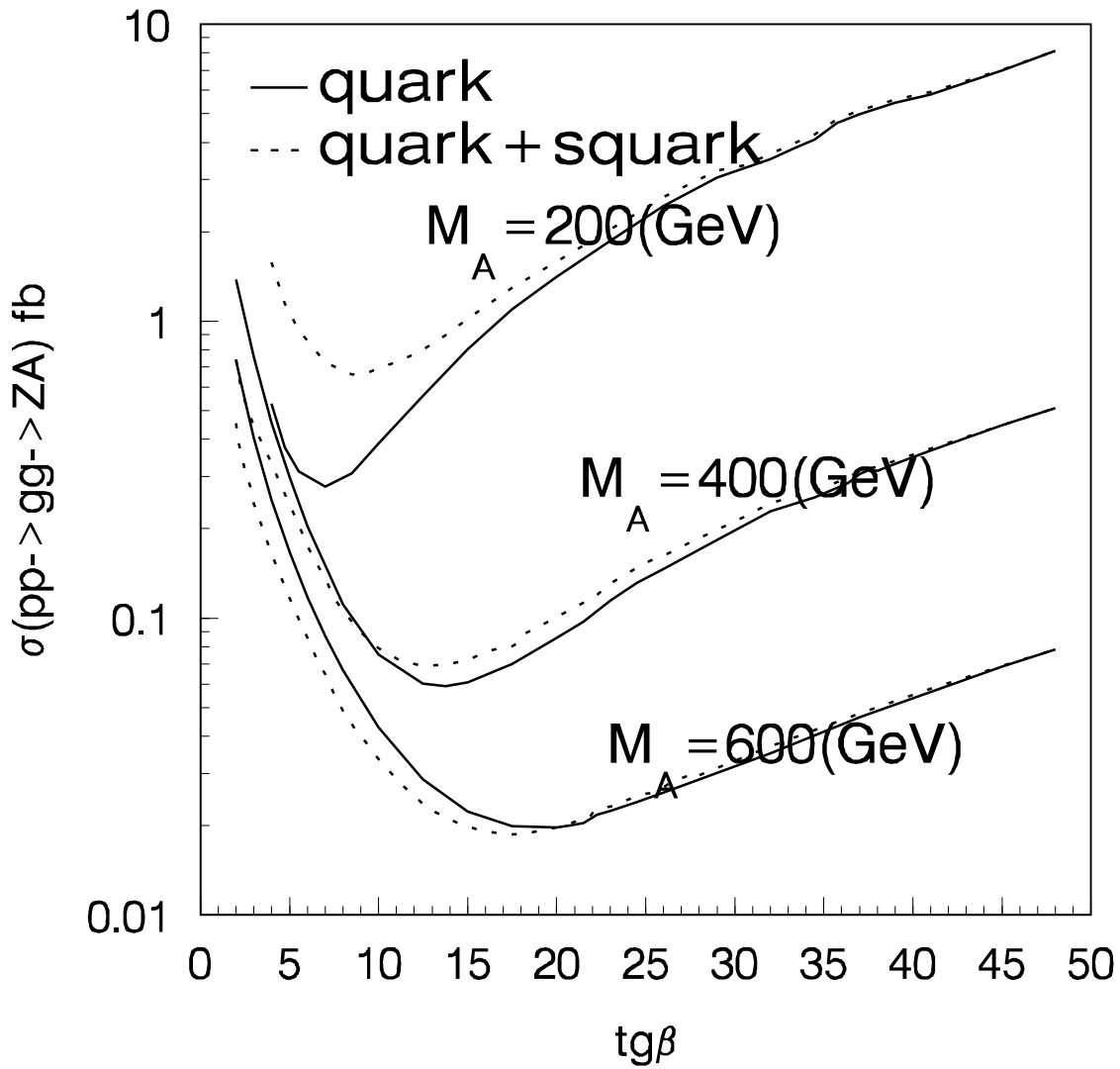


Fig.6

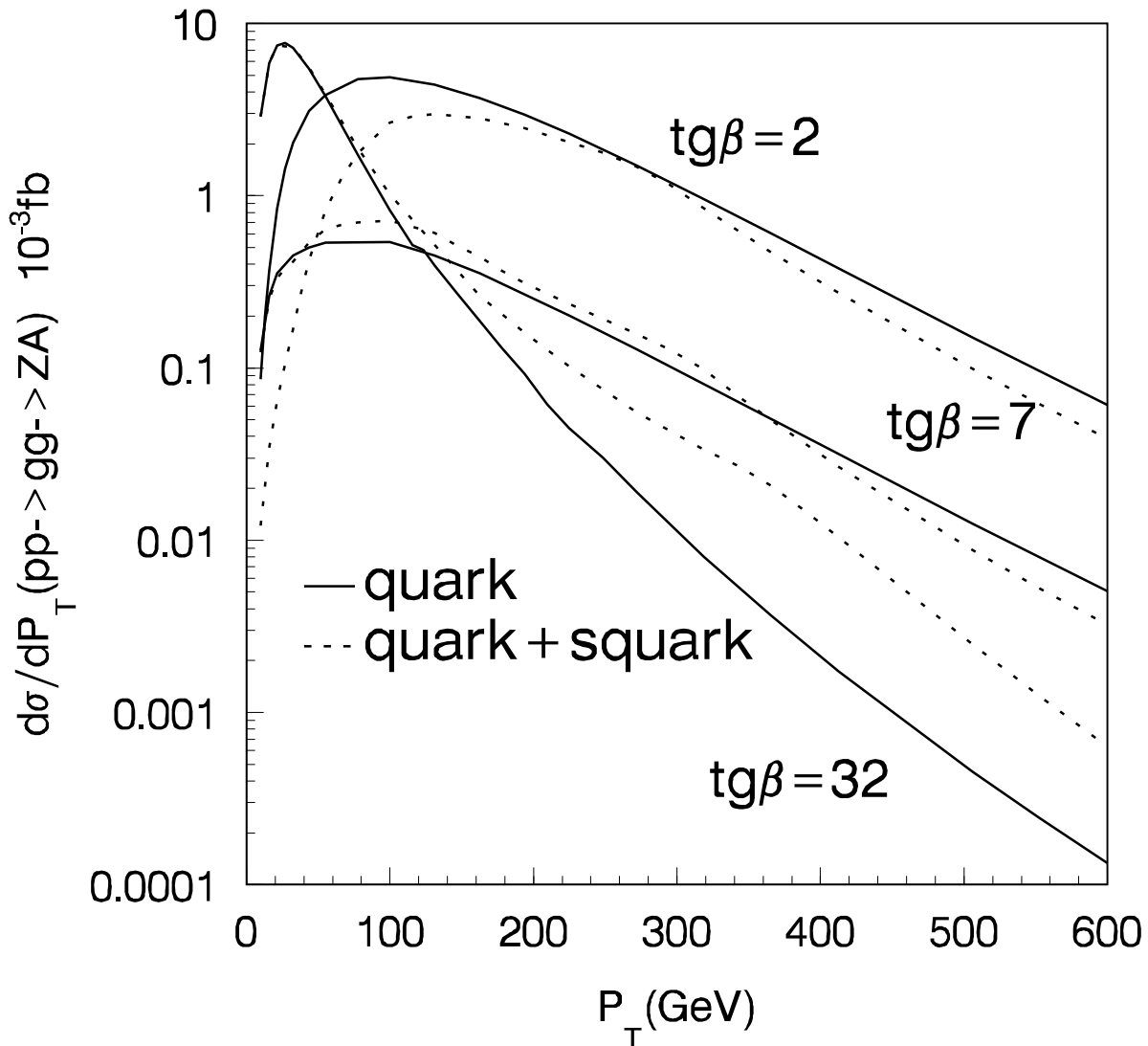


Fig.7

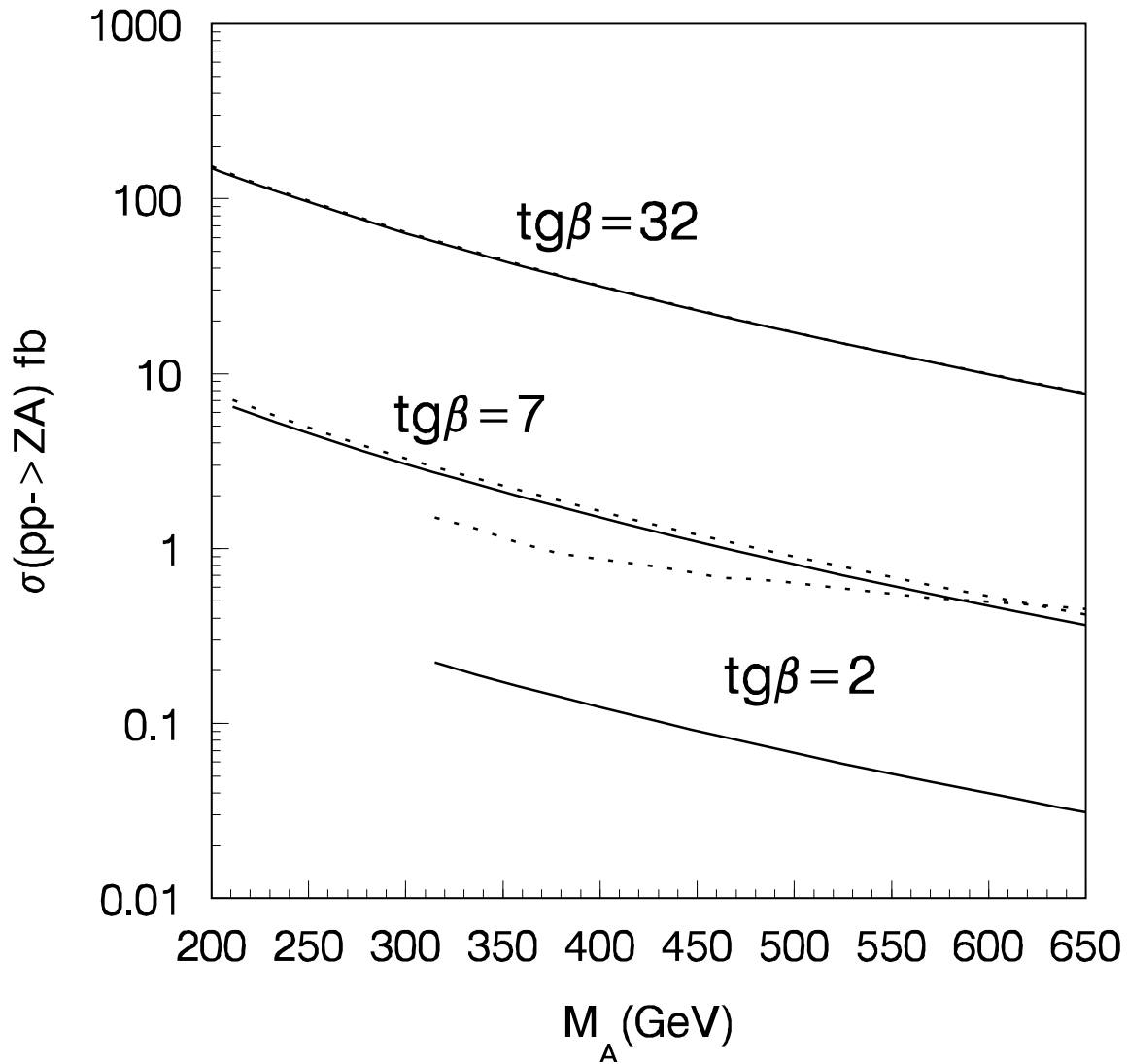


Fig.8

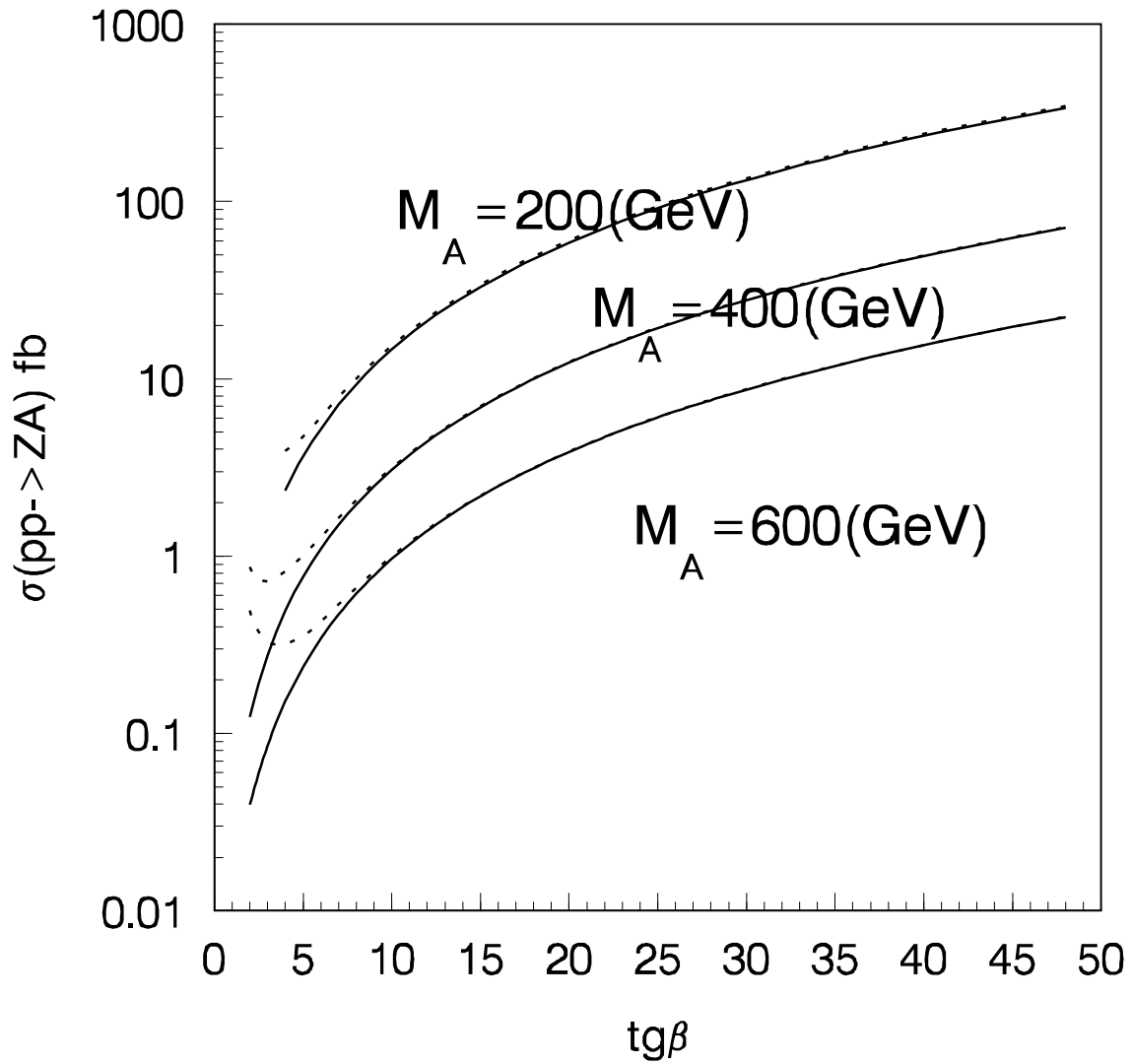


Fig.9

